HNPS Advances in Nuclear Physics

Vol 26 (2018)

HNPS2018

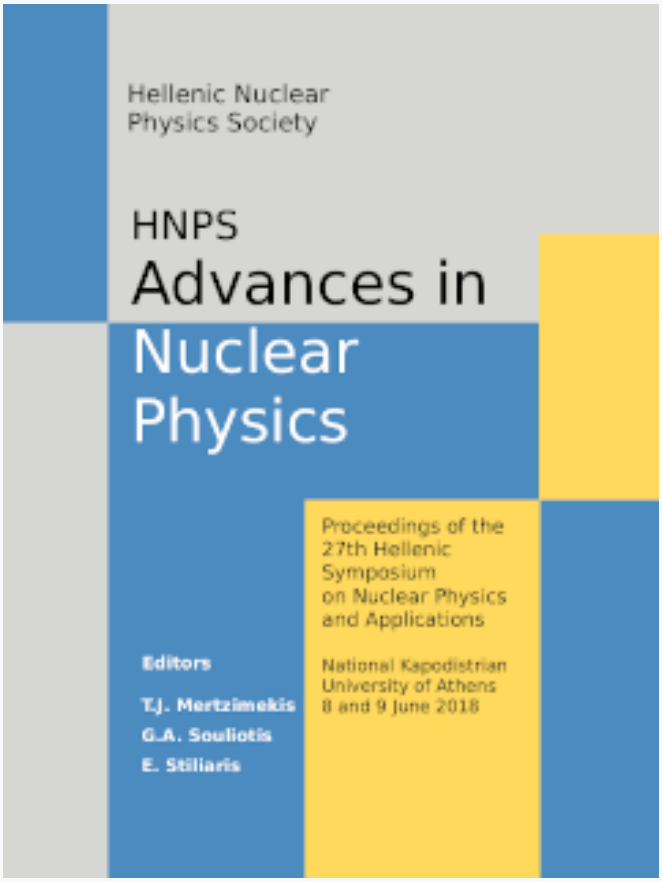

N=90 QSPT: Cerium, neodymium and samarium isotopic chains in the IBM symmetry triangle

P. Koseoglou, V. Werner, N. Pietralla, D. Bonatsos

doi: 10.12681/hnps.1793

N=90 QSPT: Cerium, neodymium and samarium isotopic chains in the IBM symmetry triangle

P. Koseoglou[1,2,*], V. Werner[1], N. Pietralla[1] , D. Bonatsos[3]

[1]*Institute for Nuclear Physics, Technische Universität Darmstadt, Schlossgartenstr. 9, 64289 Darmstadt, Germany*
[2]*GSI Helmoltzzentrum für Schwerionenforschung GmbH, Planckstr. 1, 64291 Darmstadt, Germany*
[3]*Institute of Nuclear and Particle Physics, Nuclear Center for Scientific Research "Demokritos", GR-15310 Aghia Paraskevi, Attiki, Greece*

Abstract The even-even nuclei, near the N=90 quantum shape phase transition, of cerium, neodymium and samarium isotopic chains were placed in the interacting boson model symmetry triangle. The different trajectories of the chains revealed the increasing γ-dependence from samarium to cerium by decreasing Z, which can be associated with the decreasing sharpness of the transition from spherical to deformed structures.

Keywords N=90 quantum shape phase transition, critical point, IBM-1 calculations, IBM symmetry triangle

INTRODUCTION

The even-even N=90 isotones with Z=58-64 are known to undergo a first-order quantum shape phase transition (QSPT) from spherical to deformed shapes with increasing neutron number [1,2]. In the interacting boson model (IBM) symmetry triangle [3] the three symmetries, of the three main nuclear collective shapes describing even-even nuclei in a sense of their shape and their oscillations and rotations symmetries, are placed at each vertex of the triangle as shown in Fig. 1a. The E(5) and the X(5) critical points symmetries (CPSs) are geometrical solutions of the Hamiltonian describing nuclei in the critical points of the second- and first-oder QSPT, respectively [4, 5]. E(5) is the CPS between U(5) and O(6) and X(5) between U(5) and SU(3). While the nuclear potentials of a vibrator and a symmetric rotor have one minimum, the potential of a nucleus in the critical point of the first-order QSPT presents two competing minima with a barrier between them. Along this QSPT the spherical minimum, driving the spherical forces, starts vanishing and the deformed one, driving the deformation forces, appears. The X(5) geometrical solution for the CPS neglects the barrier between the two minima and considers the potential as a square-well in the variable β and a harmonic oscillator in γ. Fingerprints for this transition region can be delivered from the analytical solution. These include the characteristic level schemes and transition strengths, or their ratios. The $R_{4/2} = E(4^+_1)/E(2^+_1) = 2.91$ and the $B_{4/2} = B(E2;4^+_1\rightarrow2^+_1)/B(E2;2^+_1\rightarrow0^+_1) = 1.58$ are benchmarks for a nucleus at the X(5) CP [5].

* Corresponding author, email: pkoseoglou@ikp.tu-darmstadt.de

Using the adopted experimental data [6], the discussed QSPT can be observed in a $R_{4/2}$ plot of these isotopes over the neutron number (Fig. 2a). The sharp transitions in the gadolinium and samarium isotopic chains from spherical nuclei ($R_{4/2}$ = 2−2.4) to deformed-ones ($R_{4/2}$ = 3−3.33) around N=90 are less pronounced in the neodymium and cerium chains. To gain additional information for the shape of the nuclei, the other fingerprint, the $B_{4/2}$ ratio ($B_{4/2}$ = 2 for spherical symmetry, $B_{4/2}$ = 1.4 for γ-rigid and γ-soft deformed), is shown in Fig. 2b as a function of the neutron number for gadolinium, samarium and neodymium isotopes. In agreement with the picture from the $R_{4/2}$ ratios, the transition from N=88 to N=90 from near spherical symmetry to quadrupole deformed shapes is sharp for gadolinium and samarium and less so for neodymium. Following the recent lifetime measurements of the 2^+_1 and 4^+_1 states of ^{148}Ce [7], within EXILL & FATIMA campaign, the $B_{4/2}$ = $B(E2;4^+_1\rightarrow2^+_1)/B(E2;2^+_1\rightarrow0^+_1)$ ratio found to be near the value of the X(5)-β^8 geometrical model [8]. All N=90 isotopes lie near the CP of the QSPT. ^{150}Nd, ^{154}Gd and ^{156}Dy near the X(5) value [5] and ^{152}Sm near the CBS for its structural parameter r_β = 0.14 [9]. In all above models the γ-softness of the nucleus is not taken into account at all, since they all consider the γ-part of the nuclear potential to be a harmonic oscillator. To include the γ-dependence IBM-1 calculations for the even-even cerium, neodymium and samarium nuclei around the QSPT were done and will be presented in the following paragraphs.

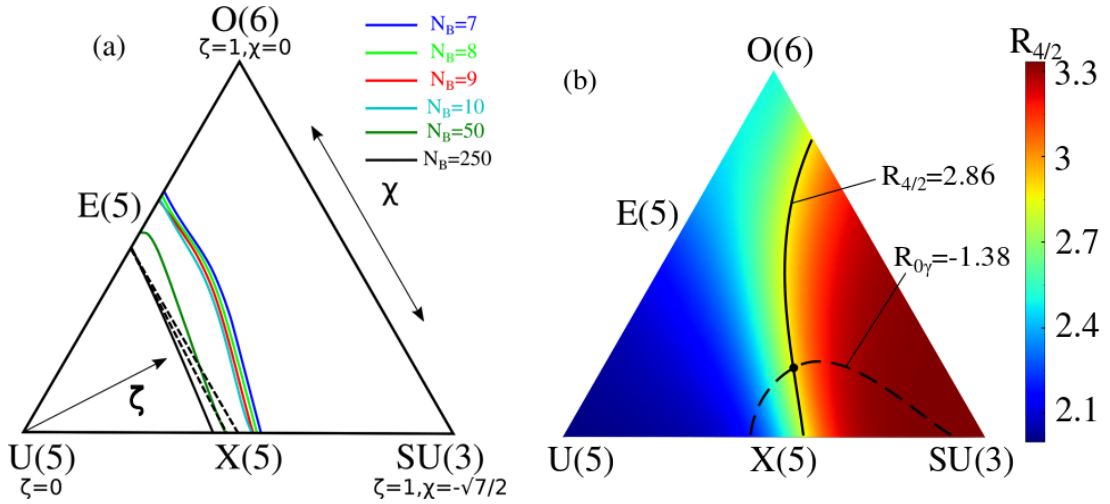

Fig. 1. (a) IBM symmetry triangle. The PT-lines for N_B =7-10, 50 and 250 (b) Placement of ^{148}Ce using the $R_{4/2}$ and $R_{0\gamma}$ contours and the experimental corresponding experimental data.

IBM - EXTENDED CONSISTENT Q FORMALISM

Whereas the geometrical models presented before, the IBM model has been proven, for the first time in the samarium isotopic chain [10], to be able to describe the collective properties of nuclei with a large range of structures by using a simplified Hamiltonian. In this simplified model, the so-called IBM-1 model, a single boson, s or d, represents a fermion pair, with no distinction between protons and neutrons [11]. For nuclei in the transition phase the Hamiltonian its more efficient, parameter-wise, to be expressed in the standard notation

of the extended consistent Q formalism (ECQF) [12, 13]

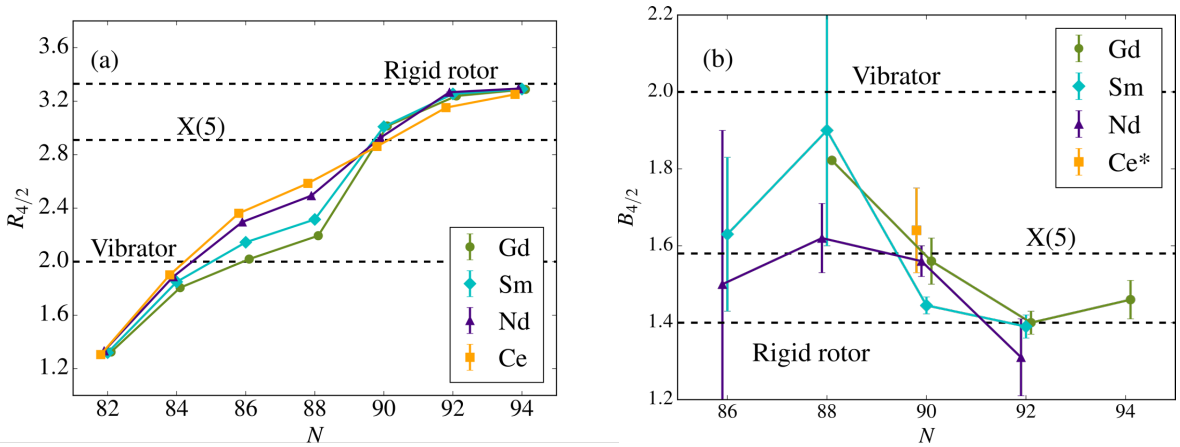

Fig. 2. Systematics over neutron number for Gd, Sm, Nd and Ce isotopic chains, (a) $R_{4/2}$ and (b) $B_{4/2}$. The data were taken from [6], except the $B_{4/2}$ value of ^{148}Ce which will be published [7].

$$H = \epsilon\, \hat{n}_d \quad - \kappa\, \hat{Q}^{\chi} \cdot \hat{Q}^{\chi} \quad (1)$$

$$H = c\,[(1-\zeta)\,\hat{n}_d - \frac{\zeta}{4N_B}\,\hat{Q}^{\chi} \cdot \hat{Q}^{\chi}], \quad (2)$$

where

$$\hat{Q}^{\chi} = (s^{\dagger}\underline{d} + d^{\dagger}\underline{s}) + \chi(\underline{d}\, d^{\dagger})^{(2)} = T(E2)/e_B \quad (3)$$

is the quadrupole operator, T(E2) is the electric quadrupole transition operator with effective boson charge e_B, c is a scaling factor and N_B the number of valence bosons. In Eq. (1) the dominant part is the first part of the equation for “more" spherical nuclei and the second part for “less” spherical nuclei, in other words for every nucleus the ratio ε/κ (or ζ) is representing the competition between the sphericity-driving and deformation-driving forces [14]. With the parameters ζ and χ the whole IBM symmetry triangle can be mapped, with ζ ∋ [0,1] and χ ∋ [−√7/2, 0], see Fig. 1a. With this parameterization the three dynamical symmetries have the following coordinates: U(5): ζ = 0 and any χ, SU(3): ζ = 1 and χ = −√7/2 and O(6): ζ = 1 and χ = 0. Spherical nuclei are described by small ζ. As ζ increases, the deformed minimum of the nuclear potential appears and is increasing against the spherical.

In Ref. [15], following the concept of the Ehrenfest classification [16], derivatives of several observables have been used in order to spot the CP of the QSPT in a finite-N system, over constant χ parameters. In our analysis the CPs were spotted by the second derivative of the binding energy. In Fig. 3 the binding energy, the first and second derivatives over ζ and for different χ parameters are plotted. The IBM-1 calculations were performed for N_B=8 with the code IBAR [17].

The location of the CP for constant N_B and χ parameter is defined by the location of the maximum in the second derivative of the binding energy as a function of ζ. So for a combination of a N_B and a χ parameter the location of the CP is defined as $\zeta_{QSPT}(N_B,\chi)$ and

can be spotted inside the IBM symmetry triangle. For constant boson number and numerous χ parameters the spots form a line inside the triangle, hereinafter referred to as phase transition line (PT-line$_{NB}$). In Fig. 1a the PT-lines for boson numbers 7-10, 50 and 250 are plotted in the IBM symmetry triangle. By increasing the N_B the PT-lines move towards the critical region in the IBM obtained in the large N_B limit from the intrinsic state formalism (dashed lines) [18]. This was also shown in Ref. [19] for the $E(6^+_1)/E(0^+_2) = 1$ line, which was shown to be a signature of the first-order phase transition in the large N_B limit.

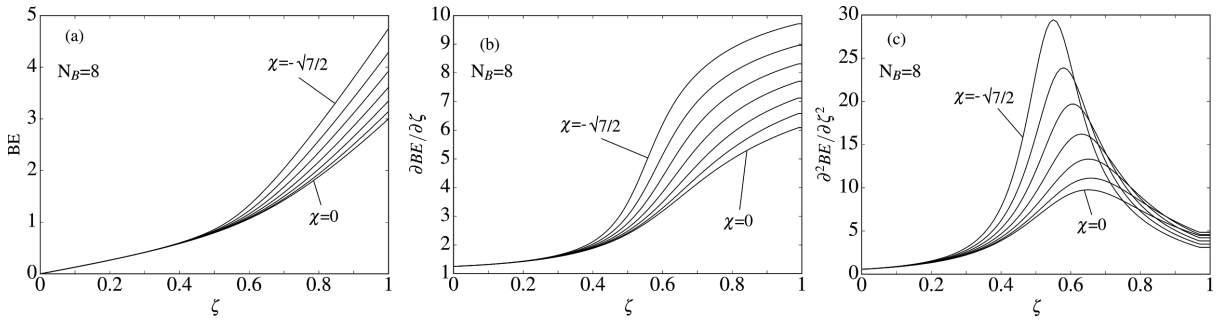

Fig. 3. (a) Binding energy, the (b) first and (c) second derivatives over ζ and for various χ parameters. The CP of the QSPT is defined by the location of the maximum in the second derivative.

Placement of isotopes in the IBM symmetry triangle

The IBM-1 calculations for various ζ and χ parameters provide a lot of observables along the triangle. In Fig. 1b the color map shows the calculated $R_{4/2}$ ratio over the whole IBM symmetry triangle for N_B=8. Contours of the observables run the whole IBM symmetry triangle. These contours together with the experimental data can be used for the placement of isotopes in the triangle [20, 21, 22, 23]. There are a lot of experimental observables which provide information for the nuclear shape. The basic observables which are also experimentally most well-known are the low-spin yarst energies, the energy of the first excited 0^+ state, $E(0^+_2)$, and the energy of the quasi-2^+_γ state, $E(2^+_\gamma)$. In this work the orthogonal crossing of two contours, connected with the basic observables, were used in order to place the isotopes in the IBM symmetry triangle. The $R_{4/2}$ contours have a vertical trajectory (in respect of the base of the triangle), and the

$$R_{0\gamma} = \frac{E(0^+_2) - E(2^+_\gamma)}{E(2^+_1)},$$

proposed in Ref. [22], have a more horizontal trajectory. The two contours corresponding on the experimental values of ^{148}Ce, $R_{4/2} = 2.86$ and $R_{0\gamma} = -1.38$, and their crossing is shown in Fig. 1b. For all cerium, neodymium and samarium isotopes in the QSPT region the crossing of the two contours is unique and allow their placement in the triangle. Their placement is shown in Fig. 4. For ^{144}Ce the $E(2^+_\gamma)$ energy is not known so the area where the nucleus is placed is defined only by the $R_{4/2}$ contour.

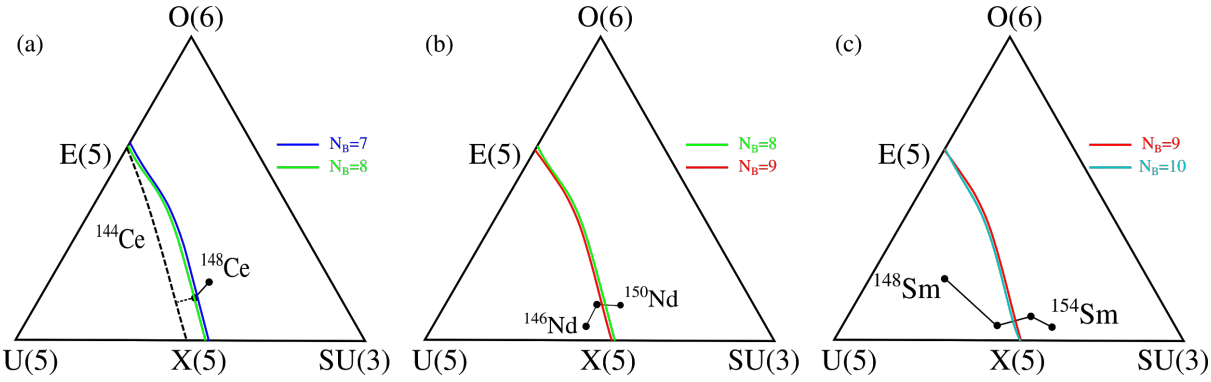

Fig. 4. Trajectories of the (a) cerium, (b) neodymium and (c) samarium isotopic chains in the IBM symmetry triangle. The γ-softness is increasing for cerium and neodymium for increasing neutron number. For samarium the trajectory stays near the base of the triangle revealing the low γ-softness along the isotopic chain for N=86-92. ^{144}Ce is placed along the black dashed line (which corresponds in the $R_{4/2}$ contour) because the $E(2^+_\gamma)$ energy is not known.

For all isotopic chains studied here the corresponding PT-line is located between the N=88 and N=90 nuclei showing the transition from spherical to deformed shapes to occur on the N=90 isotones. From the isotopic chain heading far from the base of the triangle, for cerium (for N=88-90) and neodymium (for N=88-92), we can derive the conclusion that the γ-softness of the isotopes is increasing with increasing neutron number. This picture is not seen in samarium isotopic chain which perceive the low γ-softness along the isotopic chain for N=88-92, along the QSPT.

For each isotopic chain there is a crossing χ-parameter where the line connecting the N=88 and N=90 isotopes is crossing the PT-line for the boson number of the N=90 isotope of the isotopic chain. As can be seen in Fig. 4 the crossing χ-parameter is increasing for decreasing Z (-1.13 for samarium, -1.06 for neodymium and -1 for cerium). In Fig. 5 the first derivative of the binding energy over ζ for several boson numbers and χ parameters is shown. Each line depends on a N_B and χ parameter combination (N_B,χ). Those combinations correspond on the N_B of the N=90 isotope and the crossing χ-parameter of each isotopic chain (plotted in black). Additionally the line for N_B=250 and χ=-1 is plotted in green (multiplied by 0.05 for easier comparison).

RESULTS AND DISCUSSION

In the next paragraphs we will point out two effects that are interrelated with the smoothing picture of the QSPT. First, the deviation from the thermodynamic limit due to finite N_B and second, the non-orthogonal crossing of the PT-line.

One can see in Fig. 5 that the discontinuity of a first-order phase transition is only shown in the large N_B limit (N_B=250). For small N_B it is smoothed out, less for samarium and more for neodymium and cerium. The difference between samarium, neodymium and cerium is mainly deu to the different crossing χ-parameter and less to the different N_B. Changes on the

latter are causing smaller changes in the binding energy. The last argument derives from the comparison of the Ce(8,-1) line with the two red lines in Fig. 5, which correspond to the same χ parameter for N_B=9 and 10, i.e. for neodymium and samarium isotopes on N=90.

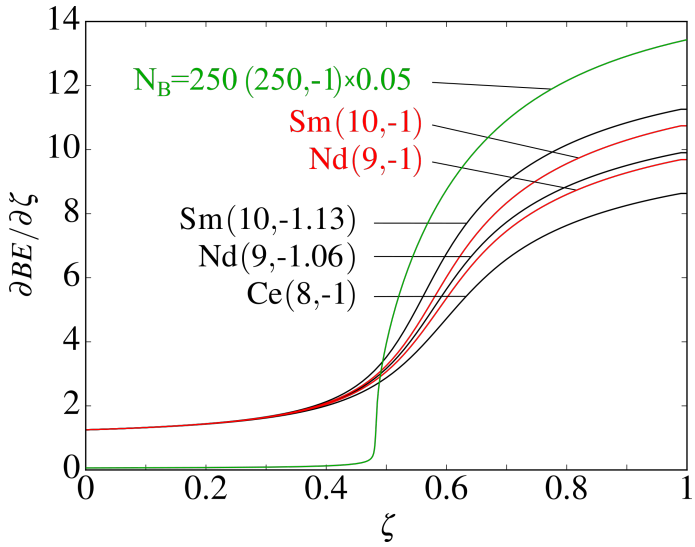

Fig. 5. First derivative of the binding energy. Each line corresponds in a N_B and χ parameter combination (N_B,χ). The N_B=250 line is multiplied by 0.05 for easier comparison.

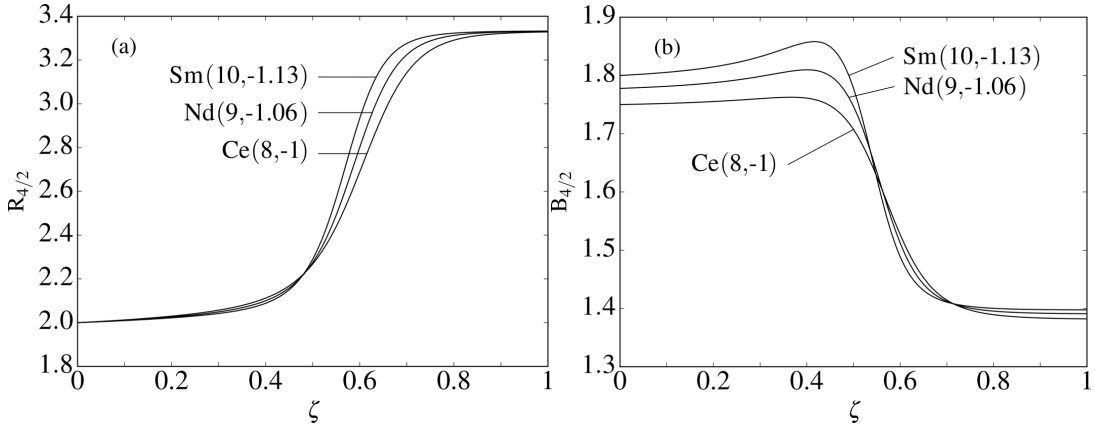

Fig. 6. (a) $R_{4/2}$ and (b) $B_{4/2}$ IBM-1 calculations. Each line depends on a N_B and χ parameter combination (N_B,χ).

As triaxiality increases from samarium to cerium, by decreasing Z, and in the same time the crossing χ-parameter is increasing, the crossing of the PT-line is less orthogonal. The smoothed out picture can be interrelated with the changes of the structural fingerprints plotted in Fig. 2, where the decreasing sharpness of the transition from spherical to deformed structures for decreasing Z is shown. Hence the crossing χ-parameter, i.e. the γ-softness, can be associated with the sharpness of the QSPT. The same picture can be seen in the $R_{4/2}$ and $B_{4/2}$ observables in the IBM-1 calculations (Fig. 6). This shows a connection between the non-orthogonal crossing of the PT-line in a finite-N system and the smoother $R_{4/2}$ and $B_{4/2}$ systematics.

Acknowledgments

We thank F. Iachello and R.F. Casten for useful discussions. This work was supported by the cooperation between TU Darmstadt and the GSI Helmholtz Center for Heavy Ion Research and by the Helmholtz Graduate School for Hadron and Ion Research for FAIR.

References

[1] R. F. Casten and N. V. Zamfir, Phys. Rev. Lett. 87 (2001) 052503, doi:10.1103/PhysRevLett.87.052503
[2] D. Warner, Nature 420 (6916) (2002) 614, doi:10.1038/420614a
[3] R. F. Casten, Nuclear Structure from a Simple Perspective, Oxford University Press, 2005.
[4] F. Iachello, Phys. Rev. Lett. 85 (2000) 3580, doi:10.1103/PhysRevLett.85.3580
[5] F. Iachello, Phys. Rev. Lett. 87 (2001) 052502, doi:10.1103/PhysRevLett.87.052502
[6] Nuclear Data Sheets [cited September 15, 2018]
[7] P. Koseoglou et al., to be published.
[8] D. Bonatsos *et al.*, Phys. Rev. C 69 (2004) 044316, doi:10.1103/PhysRevC.69.044316
[9] N. Pietralla and O. M. Gorbachenko, Phys. Rev. C 70 (2004) 011304, doi:10.1103/PhysRevC.70.011304
[10] O. Scholten, F. Iachello, A. Arima, Annals of Physics 115 (1978) 325, doi:10.1016/0003-4916(78)90159-8
[11] A. Arima, F. Iachello, Phys. Rev. Lett. 35 (1975) 1069, doi:10.1103/PhysRevLett.35.1069
[12] D.D. Warner, R.F. Casten, Phys. Rev. Lett. 48 (1982) 1385, doi:10.1103/PhysRevLett.48.1385
[13] D.D. Warner, R.F. Casten, Phys. Rev. C 28 (1983) 1798, doi:10.1103/PhysRevC.28.1798
[14] R.F. Casten, Nature Physics 2 (2006) 811, doi:10.1038/nphys451
[15] V. Werner, P. von Brentano, R. Casten, J. Jolie, Phys. Lett. B 527 (2002) 55, doi:10.1016/S0370-2693(02)01160-7
[16] L.D. Landau, E.M. Lifshitz, Statistical Physics, Course of Theoretical Physics, Vol. V, Butterworth-Heinemann, Oxford, 2001.
[17] R. Casperson, Comp. Phys. Comm. 183 (2012) 1029, doi:/10.1016/j.cpc.2011.12.024
[18] D.H. Feng, R. Gilmore and S.R. Deans, Phys. Rev. C 23,1254 (1981), doi:/10.1103/PhysRevC.23.1254
[19] D. Bonatsos *et al.*, Phys. Rev. Lett. 100, 142501, doi:/10.1103/PhysRevLett.100.142501
[20] W.-T. Chou, N.V. Zamfir, R.F. Casten, Phys. Rev. C 56 (1997) 829, doi:10.1103/PhysRevC.56.829
[21] E.A. McCutchan, N.V. Zamfir, R.F. Casten, Phys. Rev. C 69 (2004) 064306, doi:10.1103/PhysRevC.69.064306
[22] E.A. McCutchan, R.F. Casten, Phys. Rev. C 74 (2006) 057302, doi:10.1103/PhysRevC.74.057302
[23] P. Cejnar, J. Jolie, R.F. Casten, Rev. Mod. Phys. 82 (2010) 2155, doi:10.1103/RevModPhys.82.2155